Pointwise moving control for the 1-D wave equation - Numerical approximation and optimization of the support

Arthur Bottois

Arthur Bottois*

Pointwise moving control for the 1-D wave equation

Numerical approximation and optimization of the support

Abstract: We consider the exact null controllability of the 1-D wave equation with an interior pointwise control acting on a moving point $(\gamma(t))_{t\in(0,T)}$. We approximate a control of minimal norm through a mixed formulation solved by using a conformal space-time finite element method. We then introduce a gradient-type approach in order to optimize the trajectory γ of the control point. Several experiments are discussed.

Keywords: exact controllability, wave equation, pointwise control, mixed formulation, finite element approximation

1 Introduction

Let $T > 0$. We consider the linear one-dimensional wave equation in the interval $\Omega = (0, 1)$, with a pointwise control v acting on a moving point $x = \gamma(t)$, $t \in [0, T]$. The state equation reads

$$\begin{cases} y_{tt} - y_{xx} = v(t)\delta_{\gamma(t)}(x) & \text{in } Q_T = \Omega \times (0, T), \\ y = 0 & \text{on } \Sigma_T = \partial\Omega \times (0, T), \\ (y, y_t)(\cdot, 0) = (y_0, y_1) & \text{in } \Omega. \end{cases} \tag{1}$$

Here, $\delta_{\gamma(t)}$ is the Dirac measure at $x = \gamma(t)$ and γ represents the trajectory in time of the control point. The curve $\gamma : [0, T] \to \Omega$ is assumed to be piecewise C^1. We also denote by $\mathbf{H}'$ the dual space of $\mathbf{H} \coloneqq H^1(0, T)$. For $v \in \mathbf{H}'$, we refer to Section 2.1 for the well-posedness of (1).

The exact null controllability problem for (1) at time $T > 0$ is the following. *Given a trajectory $\gamma : [0, T] \to \Omega$, for any initial datum $(y_0, y_1) \in \mathbf{V} \coloneqq L^2(\Omega) \times H^{-1}(\Omega)$, find a control $v \in \mathbf{H}'$ such that the corresponding solution y of* (1)

***Corresponding author: Arthur Bottois,** Université Clermont Auvergne, Laboratoire de Mathématiques Blaise Pascal CNRS-UMR 6620, Campus des Cézeaux, F-63178 Aubière cedex, France, e-mail: arthur.bottois@uca.fr

satisfies

$$(y, y_t)(\cdot, T) = (0, 0) \quad \text{in } \Omega.$$

As a consequence of the *Hilbert uniqueness method* (HUM) introduced by J.-L. Lions [25], the controllability of (1) is equivalent to an observability inequality for the associated adjoint problem. Indeed, the state equation (1) is controllable if and only if there exists a constant $C_{\text{obs}}(\gamma) > 0$ such that

$$\|(\varphi_0, \varphi_1)\|^2_{\mathbf{W}} \leq C_{\text{obs}}(\gamma) \|\varphi(\gamma, \cdot)\|^2_{\mathbf{H}}, \quad \forall (\varphi_0, \varphi_1) \in \mathbf{W} \coloneqq H^1_0(\Omega) \times L^2(\Omega), \tag{2}$$

where $\varphi \in C([0,T]; H^1_0(\Omega)) \cap C^1([0,T]; L^2(\Omega))$ solves

$$L\varphi = 0 \text{ in } Q_T, \qquad \varphi = 0 \text{ on } \Sigma_T, \qquad (\varphi, \varphi_t)(\cdot, 0) = (\varphi_0, \varphi_1) \text{ in } \Omega. \tag{3}$$

Here, the notation $\varphi(\gamma, \cdot)$ stands for the function $\varphi(\gamma(t), t)$ with $t \in (0, T)$, while L denotes the wave operator

$$L = \partial_t^2 - \partial_x^2.$$

Under additional assumptions on γ, a proof of (2) can be found in [8]. We emphasize that the observability constant $C_{\text{obs}}(\gamma)$ depends on the control trajectory γ. In what follows, we say that γ is an *admissible trajectory* if the observability inequality (2) holds true.

In this work, we investigate the issue of the numerical approximation of the control $\widehat{v}_\gamma$ of minimal $\mathbf{H}'$-norm and the associated controlled state. We also tackle the problem of optimizing the support of control, which is done numerically by minimizing the norm $\|\widehat{v}_\gamma\|_{\mathbf{H}'}$ with respect to the trajectory γ.

Let us now mention some references related to pointwise control. This problem arises naturally in practical situations when the size of the control domain is very small compared to the size of the physical system. For a stationary control point $\gamma \equiv x_0 \in \Omega$, the controllability of (1) depends strongly on the location of x_0 [24, 26, 14]. Indeed, one can show that controllability holds if and only if the controllability time T is large enough, i.e. $T \geq 2|\Omega|$, and if there is no eigenfunction of the Dirichlet Laplacian vanishing at $x = x_0$. The constraint on T is due to the finite speed of propagation of the solution of the wave equation (1). A point x_0 satisfying the previous spectral property is referred to as a *strategic point*. Furthermore, x_0 is a strategic point if and only if it is irrational with respect to the length of Ω, making controllability very unstable. Consequently, controls acting on stationary points are usually difficult to implement in practice. It is often more convenient to control along curves for which the strategic point property holds a.e. in $[0, T]$.

For a moving control point $x = \gamma(t)$, several sufficient conditions to ensure controllability have been studied [20, 22, 8, 1]. In [22], the author proves the

existence of controls in $L^2(0,T)$ acting on a point rapidly bouncing between two positions. In [8, Proposition 4.1], the author shows, using the d'Alembert formula, that the observability inequality (2) holds under some geometric restrictions on the trajectory γ. By duality, this implies the existence of controls in $\mathbf{H}'$ for initial data in $\mathbf{V}$. The geometric requirements are related to the usual *geometric control condition* (GCC) introduced for controls acting over domains $\omega \subset \Omega$ [3, 23]. Among the constraints given to guarantee that γ is admissible, there must exist two constants $c_1, c_2 > 0$ and a finite number of subintervals $(I_j)_{0\leq j\leq J} \subset [0,T]$ such that, for each subinterval I_j, $\gamma \in C^1(I_j)$, $1 - |\gamma'|$ does not change sign in I_j and $c_1 \leq |\gamma'| \leq c_2$ in I_j. The constants appearing in the proof of the observability inequality (2) depend only on c_1 and c_2 (see [8, Remark 4.2]). Thus, it is possible to write a uniform observability inequality for trajectories in a suitable class, i.e. there exists $C > 0$ such that $C_{\text{obs}}(\gamma) \leq C$ for every γ in that class.

In the context of feedback stabilization, we mention [2]. For parabolic equations, we also mention [26, 21]. Finally, for the computation of pointwise controls for the Burgers equation, we refer to [4, 31].

The main contributions of this paper are the following. First, we use the HUM method to characterize the control $\widehat{v}$ of minimal $\mathbf{H}'$-norm, also known as the HUM control. We then turn our attention to the numerical approximation of this control and the associated controlled state. Usually (see [16, 29]), such an approximation is computed by minimizing the so-called conjugate functional $\mathcal{J}^\star_\gamma : \mathbf{W} \to \mathbb{R}$ defined by

$$\mathcal{J}^\star_\gamma(\varphi_0, \varphi_1) = \frac{1}{2}\|\varphi(\gamma,\cdot)\|^2_{\mathbf{H}} - \int_\Omega y_0\varphi_1 + \langle y_1, \varphi_0\rangle_{-1,1}, \tag{4}$$

where φ is the solution of (3) associated with (φ_0, φ_1), and $\langle\cdot,\cdot\rangle_{-1,1}$ stands for the duality product in $H^1_0(\Omega)$. Here, instead, we notice that the unconstrained minimization of $\mathcal{J}^\star_\gamma(\varphi_0, \varphi_1)$ is equivalent to the minimization of another functional $\widetilde{\mathcal{J}}^\star_\gamma(\varphi)$ (cf. (17)) over φ satisfying the constraint $L\varphi = 0$. This constraint is taken into account using a Lagrange multiplier which leads to a mixed formulation where the space and time variables are embedded. We follow the steps of [13, 9], where a similar formulation is used for controls distributed over non-cylindrical domains $q \subset Q_T$. It is worth mentioning that this space-time approach is well-adapted to our moving point situation, since we can achieve a good description of the trajectory γ embedded in a space-time mesh of Q_T. From a numerical point of view, we build a Galerkin approximation of the mixed formulation using conformal space-time finite elements. This allows to compute the optimal adjoint state $\widehat{\varphi}$, linked to the HUM control $\widehat{v}$ by the relation (9). This also gives an approximation of the Lagrange multiplier, which turns out to be the controlled state associated with $\widehat{v}$.

Another aspect of this work is the numerical optimization of the support of control. For a given initial datum $(y_0, y_1) \in \mathbf{V}$, we want to minimize the norm $\|\widehat{v}_\gamma\|_{\mathbf{H}'}$ of the HUM control $\widehat{v}_\gamma$ with respect to the trajectory γ. To do so, we consider the functional

$$J(\gamma) = \frac{1}{2}\|\widehat{v}_\gamma\|^2_{\mathbf{H}'} \tag{5}$$

and we implement a gradient-type algorithm. In order to find a descent direction at each iteration, we establish a formula for the directional derivative of J. The values of J are computed using the approximate control arising from the mixed formulation mentioned previously. We perform several numerical experiments and compare our results with those obtained in [6] for controls distributed over non-cylindrical domains $q \subset Q_T$. In the simulations, the admissible set of trajectories γ is discretized using splines functions of degree 5.

The rest of the paper is organized in three sections. First, in Section 2, we briefly give some theoretical results. Namely, we justify the existence of weak solutions for the state equation (1), and we characterize the control of minimal $\mathbf{H}'$-norm using the HUM method. We also analyse the extremal problem $\min_\gamma J(\gamma)$ (cf. (5)) and compute the directional derivative of J with respect to γ. In a second step, in Section 3, we present the space-time mixed formulation used to approximate the control and the controlled state. We also discuss some issues related to the discretization of that formulation. Finally, in Section 4, we give several numerical experiments. We illustrate the convergence of the approximated control as the discretization parameter goes to zero. For stationary control points $\gamma \equiv x_0 \in \Omega$, we illustrate the lack of controllability at non-strategic points. We also describe the gradient-type algorithm designed to optimize the support of control and discuss some results.

2 Some theoretical results

2.1 Existence of weak solutions for the state equation

The weak solution of (1) is defined by transposition (see [27]). For any $\psi \in L^1(0,T;L^2(\Omega))$, let $\varphi \in C([0,T];H^1_0(\Omega)) \cap C^1([0,T];L^2(\Omega))$ be the solution of the backward adjoint equation

$$L\varphi = \psi \text{ in } Q_T, \qquad \varphi = 0 \text{ on } \Sigma_T, \qquad (\varphi, \varphi_t)(\cdot, T) = (0,0) \text{ in } \Omega.$$

Multiplying (1) by φ and integrating by parts, we formally obtain

$$\iint_{Q_T} y\psi = \langle v, \varphi(\gamma,\cdot)\rangle_{\mathbf{H}',\mathbf{H}} - \int_\Omega y_0\varphi_t(\cdot,0) + \langle y_1, \varphi(\cdot,0)\rangle_{-1,1}, \quad \forall \psi \in L^1(0,T;L^2(\Omega)), \tag{6}$$

where $\langle\cdot,\cdot\rangle_{-1,1}$ and $\langle\cdot,\cdot\rangle_{\mathbf{H}',\mathbf{H}}$ denote respectively the duality products in $H_0^1(\Omega)$ and $\mathbf{H}$. We adopt identity (6) as the definition of the solution of (1) in the sense of transposition. One can then prove the following result (see [8, Theorem 2.1]).

Lemma 1. *Let $\gamma : [0,T] \to \Omega$ be piecewise C^1. If there exists a subdivision $(t_i)_{0\le i\le m}$ of $[0,T]$ such that, on each subinterval $[t_{i-1},t_i]$, γ is C^1 and $1-|\gamma'|$ does not change sign, there exists a unique solution y to (1) in the sense of transposition. This solution has the regularity $y \in C([0,T];L^2(\Omega))$ and $y_t \in L^2([0,T];H^{-1}(\Omega))$.*

2.2 Characterization of the HUM control

In order to give a characterization of the controls for (1), for any $(\varphi_0,\varphi_1) \in \mathbf{W}$, let φ be the solution of the adjoint equation (3). Multiplying (1) by φ and integrating by parts, we get that $v \in \mathbf{H}'$ is a control if and only if

$$\langle v, \varphi(\gamma,\cdot)\rangle_{\mathbf{H}',\mathbf{H}} = \int_\Omega y_0\varphi_1 - \langle y_1,\varphi_0\rangle_{-1,1}, \quad \forall (\varphi_0,\varphi_1) \in \mathbf{W}. \tag{7}$$

Then, by a straightforward application of the HUM method (see [8, Section 6]), we can readily characterize the control of minimal $\mathbf{H}'$-norm for (1). Let us consider the conjugate functional $\mathcal{J}_\gamma^\star$ defined in (4). If γ is an admissible trajectory, that is if the observability inequality (2) holds, we can see that $\mathcal{J}_\gamma^\star$ is continuous, strictly convex and coercive. Thus, $\mathcal{J}_\gamma^\star$ has a unique minimum point $(\widehat{\varphi}_0,\widehat{\varphi}_1) \in \mathbf{W}$, which satisfies the optimality condition

$$\langle \widehat{\varphi}(\gamma,\cdot), \varphi(\gamma,\cdot)\rangle_{\mathbf{H}} = \int_\Omega y_0\varphi_1 - \langle y_1,\varphi_0\rangle_{-1,1}, \quad \forall (\varphi_0,\varphi_1) \in \mathbf{W}, \tag{8}$$

where $\widehat{\varphi}$ and φ are the solutions of (3) associated with $(\widehat{\varphi}_0,\widehat{\varphi}_1)$ and (φ_0,φ_1) respectively. For sufficient conditions guaranteeing that a trajectory γ is admissible, we refer to [8, Theorem 2.4]. Examples of such admissible trajectories can be found in Figure 3 and [8, Section 3]. In view of (7), one can then see that the control $\widehat{v}$ of minimal $\mathbf{H}'$-norm for (1) has the following form.

Lemma 2 (HUM control)**.** *Let $\gamma \in C^1([0,T])$ piecewise. If γ is an admissible trajectory, the control $\widehat{v}$ of minimal $\mathbf{H}'$-norm for* (1) *is given by*

$$\begin{aligned}\widehat{v}(t) = &-\frac{\mathrm{d}^2}{\mathrm{d}t^2}\widehat{\varphi}(\gamma(t),t) + \widehat{\varphi}(\gamma(t),t) \\ &+ \frac{\mathrm{d}}{\mathrm{d}t}\widehat{\varphi}(\gamma(t),t)\delta_T(t) - \frac{\mathrm{d}}{\mathrm{d}t}\widehat{\varphi}(\gamma(t),t)\delta_0(t), \quad \forall t \in (0,T),\end{aligned} \tag{9}$$

where $\widehat{\varphi}$ is the solution of (3) *associated with the minimum point $(\widehat{\varphi}_0, \widehat{\varphi}_1)$ of $\mathcal{J}_\gamma^\star$, and δ_0, δ_T denote respectively the Dirac measures at $t = 0$ and $t = T$. Moreover, the norm of $\widehat{v}$ can be computed by*

$$\|\widehat{v}\|_{\mathbf{H}'}^2 = \|\widehat{\varphi}(\gamma,\cdot)\|_{\mathbf{H}}^2 = \int_0^T \varphi^2(\gamma(t),t)\,\mathrm{d}t + \int_0^T \left|\frac{\mathrm{d}}{\mathrm{d}t}\varphi(\gamma(t),t)\right|^2 \mathrm{d}t. \tag{10}$$

2.3 Optimization of the support of control

We focus here on the optimization of the control trajectory. More precisely, for $(y_0, y_1) \in \mathbf{V}$ fixed, we want to minimize the norm $\|\widehat{v}\|_{\mathbf{H}'}$ (cf. (10)) of the HUM control with respect to the curve γ, i.e. solve

$$\min_{\gamma\in\mathcal{G}} J(\gamma), \quad \text{where } J(\gamma) = \frac{1}{2}\int_0^T \varphi^2(\gamma(t),t)\,\mathrm{d}t + \frac{1}{2}\int_0^T \left|\frac{\mathrm{d}}{\mathrm{d}t}\varphi(\gamma(t),t)\right|^2 \mathrm{d}t, \tag{11}$$

and where φ is the solution of (3) associated with the minimum point (φ_0, φ_1) of $\mathcal{J}_\gamma^\star$. The admissible set $\mathcal{G}$ is composed of smooth trajectories, typically of class $C^2([0,T])$. We also require that the observability inequality (2) holds uniformly on $\mathcal{G}$, meaning that there exists $C > 0$ such that $C_{\mathrm{obs}}(\gamma) \leq C$ for every $\gamma \in \mathcal{G}$. This property can be achieved with the hypotheses of [8, Theorem 2.4]. In Section 4, we discretize $\mathcal{G}$ using the space $\mathcal{S}_5$ of degree 5 splines, adapted to a fixed regular subdivision of $[0,T]$.

As it stands, we do not know if the extremal problem (11) is well-posed. To establish the lower semi-continuity of J, it could be possible to exploit the works [18, 19] where, in the context of the heat equation, the authors consider a shape optimization problem with respect to a curve. In the process, it might be necessary to have a more regular control, which would probably require more regular initial data (y_0, y_1) (see [15]).

Moreover, a longer trajectory γ allows intuitively a smaller cost of control. Consequently, to give more sense to the problem, we penalize the length $L(\gamma)$ of the curve γ. Similarly, in order to avoid too fast variations of the trajectory, we

also regularize the "curvature" γ''. A similar strategy has been introduced and discussed in [6]. Thus, for $\varepsilon > 0$ small enough, $\eta > 0$ large enough and $\overline{L} \geq T$ fixed, we consider the following regularized-penalized extremal problem

$$\min_{\gamma \in \mathcal{G}} J_{\varepsilon,\eta}(\gamma), \quad \text{where } J_{\varepsilon,\eta}(\gamma) = J(\gamma) + \frac{\varepsilon}{2}\|\gamma''\|^2_{L^2(0,T)} + \frac{\eta}{2}\Big((L(\gamma) - \overline{L})^+\Big)^2, \quad (12)$$

and where $(\cdot)^+$ stands for the positive part.

We solve this problem numerically in Section 4, using a gradient-type algorithm. In order to evaluate a descent direction for $J_{\varepsilon,\eta}$ at each iteration of the algorithm, we compute the derivatives of J and $J_{\varepsilon,\eta}$ with respect to γ.

Lemma 3. *Let $\gamma \in C^2([0,T])$ be an admissible trajectory and let $\overline{\gamma} \in C^2([0,T])$ be a perturbation. The directional derivative of J at γ in the direction $\overline{\gamma}$, defined by $\mathrm{d}J(\gamma;\overline{\gamma}) \coloneqq \lim_{\nu \to 0} \dfrac{J(\gamma + \nu\overline{\gamma}) - J(\gamma)}{\nu}$, reads as follows*

$$\begin{aligned}\mathrm{d}J(\gamma;\overline{\gamma}) = &- \int_0^T \varphi(\gamma(t),t)\varphi_x(\gamma(t),t)\overline{\gamma}(t)\,\mathrm{d}t \\ &- \int_0^T \frac{\mathrm{d}}{\mathrm{d}t}\varphi(\gamma(t),t)\frac{\mathrm{d}}{\mathrm{d}t}\Big(\varphi_x(\gamma(t),t)\overline{\gamma}(t)\Big)\mathrm{d}t,\end{aligned}$$

where φ is the solution of (3) associated with the minimum point (φ_0,φ_1) of $\mathcal{J}^\star_\gamma$. Similarly, the directional derivative of $J_{\varepsilon,\eta}$ at γ in the direction $\overline{\gamma}$ is given by

$$\mathrm{d}J_{\varepsilon,\eta}(\gamma;\overline{\gamma}) = \mathrm{d}J(\gamma;\overline{\gamma}) + \varepsilon\langle\gamma'',\overline{\gamma}''\rangle_{L^2(0,T)} + \eta(L(\gamma) - \overline{L})^+\mathrm{d}L(\gamma;\overline{\gamma}),$$

where

$$L(\gamma) = \int_0^T \sqrt{1+\gamma'^2} \qquad \text{and} \qquad \mathrm{d}L(\gamma;\overline{\gamma}) = \int_0^T \frac{\gamma'}{\sqrt{1+\gamma'^2}}\overline{\gamma}'.$$

Proof. We provide only a formal proof. Rigorous demonstrations of similar lemmas can be found in [30, 6], for controls distributed over domains $q \subset Q_T$. For any admissible trajectory $\gamma \in C^2([0,T])$ and any perturbation $\overline{\gamma} \in C^2([0,T])$, we get

$$\begin{aligned}\mathrm{d}J(\gamma;\overline{\gamma}) = &\int_0^T \varphi(\gamma(t),t)\Big(\varphi'(\gamma(t),t) + \varphi_x(\gamma(t),t)\overline{\gamma}(t)\Big)\mathrm{d}t \\ &+ \int_0^T \frac{\mathrm{d}}{\mathrm{d}t}\varphi(\gamma(t),t)\frac{\mathrm{d}}{\mathrm{d}t}\Big(\varphi'(\gamma(t),t) + \varphi_x(\gamma(t),t)\overline{\gamma}(t)\Big)\mathrm{d}t.\end{aligned} \quad (13)$$

Here, φ' denotes the derivative of φ with respect to γ. To simplify (13), we differentiate the optimality condition (8) with respect to γ. It gives

$$\int_0^T \Big(\varphi'(\gamma(t),t) + \varphi_x(\gamma(t),t)\overline{\gamma}(t)\Big)\psi(\gamma(t),t)\,\mathrm{d}t + \int_0^T \varphi(\gamma(t),t)\psi_x(\gamma(t),t)\overline{\gamma}(t)\,\mathrm{d}t + \int_0^T \frac{\mathrm{d}}{\mathrm{d}t}\Big(\varphi'(\gamma(t),t) + \varphi_x(\gamma(t),t)\overline{\gamma}(t)\Big)\frac{\mathrm{d}}{\mathrm{d}t}\psi(\gamma(t),t)\,\mathrm{d}t + \int_0^T \frac{\mathrm{d}}{\mathrm{d}t}\varphi(\gamma(t),t)\frac{\mathrm{d}}{\mathrm{d}t}\Big(\psi_x(\gamma(t),t)\overline{\gamma}(t)\Big)\mathrm{d}t = 0, \quad \forall(\psi_0,\psi_1)\in\mathbf{W},$$

where ψ is the solution of (3) associated with (ψ_0,ψ_1). Evaluating the previous expression for $(\psi_0,\psi_1) = (\varphi_0,\varphi_1)$, we can eliminate the derivative φ' from (13) and obtain the announced result. □

3 Mixed formulation

In this section, in order to approximate the HUM control for (1) and the associated controlled state, we present a space-time mixed formulation based on the optimality condition (8). We follow the steps of [9, Section 3.1], where a similar formulation is built for controls distributed over domains $q \subset Q_T$. From a numerical point of view, this space-time formulation is very appropriate for the moving point situation considered in this work. Indeed, after the discretization step, we solve the formulation using a space-time triangular mesh, which is constructed from boundary vertices placed on the border of Q_T and on the curve γ.

3.1 Mixed formulation

We start by a lemma extending the observability inequality (2). For this, we first need to introduce the functional space

$$\mathbf{\Phi} \coloneqq \Big\{\varphi \in C([0,T];H_0^1(\Omega)) \cap C^1([0,T];L^2(\Omega)); \quad L\varphi \in L^2(0,T;L^2(\Omega))\Big\}.$$

Lemma 4 (Generalized observability inequality)**.** *Let $\gamma \in C^1([0,T])$ piecewise. If γ is an admissible trajectory, there exists a constant $\widetilde{C}_{\mathrm{obs}}(\gamma) > 0$ such that*

$$\|(\varphi,\varphi_t)(\cdot,0)\|_{\mathbf{W}}^2 \le \widetilde{C}_{\mathrm{obs}}(\gamma)\Big(\|\varphi(\gamma,\cdot)\|_{\mathbf{H}}^2 + \|L\varphi\|_{L^2(0,T;L^2(\Omega))}^2\Big), \quad \forall\varphi\in\mathbf{\Phi}. \tag{14}$$

Proof. Let $\varphi \in \mathbf{\Phi}$. We can decompose $\varphi = \psi_1 + \psi_2$, where $\psi_1, \psi_2 \in \mathbf{\Phi}$ solve

$$\begin{cases} L\psi_1 = 0 \quad \text{in } Q_T, \quad \psi_1 = 0 \text{ on } \Sigma_T, \quad (\psi_1, \psi_{1,t})(\cdot,0) = (\varphi, \varphi_t)(\cdot,0) \text{ in } \Omega, \\ L\psi_2 = L\varphi \text{ in } Q_T, \quad \psi_2 = 0 \text{ on } \Sigma_T, \quad (\psi_2, \psi_{2,t})(\cdot,0) = (0,0) \qquad \text{in } \Omega. \end{cases}$$

From Duhamel's principle and the conservation of energy, one can show (see [8, Section 5]) the following so-called hidden regularity property for ψ_2, there exists a constant $c(\gamma) > 0$ such that

$$\|\psi_2(\gamma,\cdot)\|^2_{\mathbf{H}} \leq c(\gamma)\|L\varphi\|^2_{L^2(0,T;L^2(\Omega))}. \tag{15}$$

Combining (2) for ψ_1 and (15) for ψ_2, we obtain

$$\begin{aligned} \|(\varphi,\varphi_t)(\cdot,0)\|^2_{\mathbf{W}} = \|(\psi_1,\psi_{1,t})(\cdot,0)\|^2_{\mathbf{W}} &\leq C_{\mathrm{obs}}(\gamma)\|\psi_1(\gamma,\cdot)\|^2_{\mathbf{H}} \\ &\leq 2C_{\mathrm{obs}}(\gamma)\Big(\|\varphi(\gamma,\cdot)\|^2_{\mathbf{H}} + \|\psi_2(\gamma,\cdot)\|^2_{\mathbf{H}}\Big) \\ &\leq \widetilde{C}_{\mathrm{obs}}(\gamma)\Big(\|\varphi(\gamma,\cdot)\|^2_{\mathbf{H}} + \|L\varphi\|^2_{L^2(0,T;L^2(\Omega))}\Big). \end{aligned}$$

□

As for (2), it is possible to find a class of admissible trajectories γ such that the generalized observability inequality (14) holds uniformly (see [8, Theorem 2.4]), i.e. there exists $\widetilde{C} > 0$ such that $\widetilde{C}_{\mathrm{obs}}(\gamma) \leq \widetilde{C}$ for every γ in that class. In addition, the inequality (14) implies the following property on the space $\mathbf{\Phi}$.

Lemma 5. *Let $\gamma \in C^1([0,T])$ piecewise. If γ is an admissible trajectory, the space $\mathbf{\Phi}$ is a Hilbert space with the inner product*

$$\langle \varphi, \overline{\varphi} \rangle_{\mathbf{\Phi}} = \langle \varphi(\gamma,\cdot), \overline{\varphi}(\gamma,\cdot) \rangle_{\mathbf{H}} + \tau \langle L\varphi, L\overline{\varphi} \rangle_{L^2(0,T;L^2(\Omega))}, \quad \forall \varphi, \overline{\varphi} \in \mathbf{\Phi}, \tag{16}$$

for $\tau > 0$ fixed.

Proof. The semi-norm $\|\cdot\|_{\mathbf{\Phi}}$ associated with the inner product is trivially a norm in view of the generalized observability inequality (14). It remains to prove that $\mathbf{\Phi}$ is complete with respect to this norm. Let $(\varphi_k)_{k\geq 1} \subset \mathbf{\Phi}$ be a Cauchy sequence for the norm $\|\cdot\|_{\mathbf{\Phi}}$. So, there exists $f \in L^2(0,T;L^2(\Omega))$ such that $L\varphi_k \to f$ in $L^2(0,T;L^2(\Omega))$. As a consequence of (14), there also exists $(\varphi_0,\varphi_1) \in \mathbf{W}$ such that $(\varphi_k,\varphi_{k,t})(\cdot,0) \to (\varphi_0,\varphi_1)$ in $\mathbf{W}$. Therefore, $(\varphi_k)_{k\geq 1}$ can be considered as a sequence of solutions of the wave equation with convergent initial data and convergent right-hand sides. By the continuous dependence of the solution of the wave equation on the data, $\varphi_k \to \varphi$ in $C([0,T];H^1_0(\Omega)) \cap C^1([0,T];L^2(\Omega))$, where φ is the solution of the wave equation with initial datum $(\varphi_0,\varphi_1) \in \mathbf{W}$ and right-hand side $f \in L^2(0,T;L^2(\Omega))$. Thus, $\varphi \in \mathbf{\Phi}$. □

We can now turn to the set-up of the mixed formulation. In order to avoid the minimization of the conjugate functional $\mathcal{J}_\gamma^\star$ (cf. (4)) with respect to (φ_0, φ_1), we remark that the solution φ of (3) is completely and uniquely determined by the initial datum (φ_0, φ_1). Then, the main idea of the reformulation is to keep φ as main variable and consider instead the minimization of

$$\widetilde{\mathcal{J}}_\gamma^\star(\varphi) = \frac{1}{2}\|\varphi(\gamma,\cdot)\|_{\mathbf{H}}^2 - \int_\Omega y_0\varphi_t(\cdot,0) + \langle y_1, \varphi(\cdot,0)\rangle_{-1,1} \tag{17}$$

over

$$\mathbf{\Phi}_0 \coloneqq \Big\{\varphi \in \mathbf{\Phi}; \quad L\varphi = 0 \in L^2(0,T;L^2(\Omega))\Big\}.$$

Indeed, we clearly have

$$\min_{(\varphi_0,\varphi_1)\in\mathbf{W}} \mathcal{J}_\gamma^\star(\varphi_0,\varphi_1) = \mathcal{J}_\gamma^\star(\widehat{\varphi}_0,\widehat{\varphi}_1) = \widetilde{\mathcal{J}}_\gamma^\star(\widehat{\varphi}) = \min_{\varphi\in\mathbf{\Phi}_0} \widetilde{\mathcal{J}}_\gamma^\star(\varphi),$$

where $\widehat{\varphi}$ is the solution of (3) associated with the minimum point $(\widehat{\varphi}_0, \widehat{\varphi}_1)$ of $\mathcal{J}_\gamma^\star$. Besides, the minimum point $\widehat{\varphi}$ of $\widetilde{\mathcal{J}}_\gamma^\star$ is unique. So, the new variable is the function φ with the constraint $L\varphi = 0$ in $L^2(0,T;L^2(\Omega))$. To deal with this constraint, we introduce a Lagrange multiplier $\lambda \in \mathbf{\Lambda} \coloneqq L^2(0,T;L^2(\Omega))$. We thus consider the following problem: find $(\varphi,\lambda) \in \mathbf{\Phi}\times\mathbf{\Lambda}$ solution of

$$\left\{\begin{array}{rl} a(\varphi,\overline{\varphi}) - b(\overline{\varphi},\lambda) = \ell(\overline{\varphi}), & \forall \overline{\varphi} \in \mathbf{\Phi}, \\ b(\varphi,\overline{\lambda}) = 0, & \forall \overline{\lambda} \in \mathbf{\Lambda}, \end{array}\right. \tag{18}$$

where we have set

$$\begin{aligned} &a : \mathbf{\Phi}\times\mathbf{\Phi} \to \mathbb{R}, && a(\varphi,\overline{\varphi}) = \langle \varphi(\gamma,\cdot), \overline{\varphi}(\gamma,\cdot)\rangle_{\mathbf{H}}, \\ &b : \mathbf{\Phi}\times\mathbf{\Lambda} \to \mathbb{R}, && b(\varphi,\lambda) = \langle L\varphi,\lambda\rangle_{L^2(0,T;L^2(\Omega))}, \\ &\ell : \mathbf{\Phi} \to \mathbb{R}, && \ell(\varphi) = \int_\Omega y_0\varphi_t(\cdot,0) - \langle y_1,\varphi(\cdot,0)\rangle_{-1,1}. \end{aligned}$$

The introduction of this problem is justified by the result below.

Theorem 1 (Mixed formulation)**.** *Let $\gamma \in C^1([0,T])$ piecewise. If γ is an admissible trajectory, we have the following properties;*

- *The mixed formulation* (18) *is well-posed.*
- *The unique solution $(\varphi,\lambda) \in \mathbf{\Phi}\times\mathbf{\Lambda}$ is the unique saddle point of the Lagrangian $\mathcal{L} : \mathbf{\Phi}\times\mathbf{\Lambda} \to \mathbb{R}$ defined by*

$$\mathcal{L}(\varphi,\lambda) = \frac{1}{2}a(\varphi,\varphi) - b(\varphi,\lambda) - \ell(\varphi).$$

- *The optimal function φ is the minimum point of $\widetilde{\mathcal{J}}_\gamma^\star$ over $\mathbf{\Phi}_0$. Besides, the optimal function $\lambda \in \mathbf{\Lambda}$ is the solution of the controlled wave equation* (1)*, with the control v associated with φ (cf.* (9)*).*

Proof. We easily check that the bilinear form a is continuous over $\mathbf{\Phi}\times\mathbf{\Phi}$, symmetric and positive. Similarly, we check that the bilinear form b is continuous over $\mathbf{\Phi}\times\mathbf{\Lambda}$. Furthermore, the continuity of the linear form ℓ over $\mathbf{\Phi}$ is a direct consequence of the generalized observability inequality (14),

$$|\ell(\varphi)| \leq \|(y_0,y_1)\|_{\mathbf{V}}\sqrt{2\widetilde{C}_{\rm obs}(\gamma)\max(1,\tau^{-1})}\|\varphi\|_{\mathbf{\Phi}}, \quad \forall\varphi\in\mathbf{\Phi}.$$

Therefore, to prove the well-posedness of the mixed formulation (18), we only need to check the following two properties (see [7]).

- The form a is coercive on the kernel $\mathcal{N}(b) \coloneqq \big\{\varphi\in\mathbf{\Phi};\ b(\varphi,\lambda)=0,\ \forall\lambda\in\mathbf{\Lambda}\big\}$.
- The form b satisfies the usual "inf-sup" condition over $\mathbf{\Phi}\times\mathbf{\Lambda}$, i.e. there exists a constant $\delta>0$ such that

$$\inf_{\lambda\in\mathbf{\Lambda}}\sup_{\varphi\in\mathbf{\Phi}}\frac{b(\varphi,\lambda)}{\|\varphi\|_{\mathbf{\Phi}}\|\lambda\|_{\mathbf{\Lambda}}}\geq\delta. \tag{19}$$

From the definition of a, the first point is clear. Indeed, for any $\varphi\in\mathcal{N}(b)=\mathbf{\Phi}_0$, $a(\varphi,\varphi)=\|\varphi\|^2_{\mathbf{\Phi}}$. We now check the inf-sup condition (19). For any $\lambda_0\in\mathbf{\Lambda}$, we define the unique element $\varphi_0\in\mathbf{\Phi}$ such that

$$L\varphi_0=\lambda_0 \text{ in } Q_T, \qquad \varphi_0=0 \text{ on } \Sigma_T, \qquad (\varphi_0,\varphi_{0,t})(\cdot,0)=(0,0) \text{ in } \Omega.$$

It implies $b(\varphi_0,\lambda_0)=\|\lambda_0\|^2_{\mathbf{\Lambda}}$ and

$$\sup_{\varphi\in\mathbf{\Phi}}\frac{b(\varphi,\lambda_0)}{\|\varphi\|_{\mathbf{\Phi}}\|\lambda_0\|_{\mathbf{\Lambda}}}\geq\frac{b(\varphi_0,\lambda_0)}{\|\varphi_0\|_{\mathbf{\Phi}}\|\lambda_0\|_{\mathbf{\Lambda}}}=\frac{\|\lambda_0\|_{\mathbf{\Lambda}}}{\sqrt{\|\varphi_0(\gamma,\cdot)\|^2_{\mathbf{H}}+\tau\|\lambda_0\|^2_{\mathbf{\Lambda}}}}.$$

We then use the following estimate (see [8, Section 5]), there exists a constant $c(\gamma)>0$ such that

$$\|\varphi_0(\gamma,\cdot)\|^2_{\mathbf{H}}\leq c(\gamma)\|\lambda_0\|^2_{\mathbf{\Lambda}}.$$

Combining the two previous inequalities, we obtain

$$\sup_{\varphi\in\mathbf{\Phi}}\frac{b(\varphi,\lambda_0)}{\|\varphi\|_{\mathbf{\Phi}}\|\lambda_0\|_{\mathbf{\Lambda}}}\geq\frac{1}{\sqrt{c(\gamma)+\tau}}, \quad \forall\lambda_0\in\mathbf{\Lambda}.$$

Hence, the inequality (19) holds with $\delta=(c(\gamma)+\tau)^{-\frac{1}{2}}$.

The second point of the theorem is due to the symmetry and positivity of the bilinear form a. Regarding the third point, the equality $b(\varphi,\overline{\lambda})=0$ for all $\overline{\lambda}\in\mathbf{\Lambda}$ implies that $L\varphi=0$ in $L^2(0,T;L^2(\Omega))$. Besides, for $\overline{\varphi}\in\mathbf{\Phi}_0$, the first equation of (18) gives $a(\varphi,\overline{\varphi})=\ell(\overline{\varphi})$. So, if $(\varphi,\lambda)\in\mathbf{\Phi}\times\mathbf{\Lambda}$ solves the mixed formulation, then $\varphi\in\mathbf{\Phi}_0$ and $\mathcal{L}(\varphi,\lambda)=\widetilde{\mathcal{J}}^\star_\gamma(\varphi)$. Moreover, again due to the symmetry and positivity

of a, the function φ is the minimum point of $\widetilde{\mathcal{J}}_\gamma^\star$ over $\mathbf{\Phi}_0$. Indeed, for any $\overline{\varphi} \in \mathbf{\Phi}_0$, we have

$$\widetilde{\mathcal{J}}_\gamma^\star(\varphi) = -\frac{1}{2}a(\varphi,\varphi) \leq \frac{1}{2}a(\overline{\varphi},\overline{\varphi}) - a(\varphi,\overline{\varphi}) = \frac{1}{2}a(\overline{\varphi},\overline{\varphi}) - \ell(\overline{\varphi}) = \widetilde{\mathcal{J}}_\gamma^\star(\overline{\varphi}).$$

Finally, the first equation of (18) reads

$$\langle \varphi(\gamma,\cdot), \overline{\varphi}(\gamma,\cdot)\rangle_{\mathbf{H}} - \langle L\overline{\varphi}, \lambda\rangle_{\mathbf{\Lambda}} = \int_\Omega y_0 \overline{\varphi}_t(\cdot,0) - \langle y_1, \overline{\varphi}(\cdot,0)\rangle_{-1,1}, \quad \forall \overline{\varphi} \in \mathbf{\Phi}.$$

Since the control v of minimal $\mathbf{H}'$-norm is given by (9), we get

$$\iint_{Q_T} \lambda L\overline{\varphi} = \langle v, \overline{\varphi}(\gamma,\cdot)\rangle_{\mathbf{H}',\mathbf{H}} - \int_\Omega y_0 \overline{\varphi}_t(\cdot,0) + \langle y_1, \overline{\varphi}(\cdot,0)\rangle_{-1,1}, \quad \forall \overline{\varphi} \in \mathbf{\Phi}.$$

But this means that λ is solution in a weak sense of the wave equation (1) associated with the initial datum $(y_0, y_1) \in \mathbf{V}$ and the control $v \in \mathbf{H}'$. □

Consequently, the search of the HUM control for (1) is reduced to the resolution of the mixed formulation (18), or equivalently to the search of the saddle point of $\mathcal{L}$. Moreover, for numerical purposes, it is convenient to "augment" the Lagrangian $\mathcal{L}$ and to consider instead the Lagrangian $\mathcal{L}_r$ defined, for any $r > 0$, by

$$\begin{cases} \mathcal{L}_r(\varphi,\lambda) = \dfrac{1}{2}a_r(\varphi,\varphi) - b(\varphi,\lambda) - \ell(\varphi), \\ a_r(\varphi,\overline{\varphi}) = a(\varphi,\overline{\varphi}) + r\langle L\varphi, L\overline{\varphi}\rangle_{L^2(0,T;L^2(\Omega))}. \end{cases}$$

Since $a(\varphi,\varphi) = a_r(\varphi,\varphi)$ for $\varphi \in \mathbf{\Phi}_0$, the Lagrangians $\mathcal{L}$ and $\mathcal{L}_r$ share the same saddle point.

3.2 Discretization

We now turn to the discretization of the mixed formulation (18). Let $(\mathbf{\Phi}_h)_{h>0} \subset \mathbf{\Phi}$ and $(\mathbf{\Lambda}_h)_{h>0} \subset \mathbf{\Lambda}$ be two families of finite-dimensional spaces. For any $h > 0$, we introduce the following approximated problem: find $(\varphi_h, \lambda_h) \in \mathbf{\Phi}_h \times \mathbf{\Lambda}_h$ solution of

$$\left\{ \begin{array}{rcll} a_r(\varphi_h,\overline{\varphi}_h) - b(\overline{\varphi}_h,\lambda_h) &=& \ell(\overline{\varphi}_h), & \forall \overline{\varphi}_h \in \mathbf{\Phi}_h, \\ b(\varphi_h,\overline{\lambda}_h) &=& 0, & \forall \overline{\lambda}_h \in \mathbf{\Lambda}_h. \end{array} \right. \tag{20}$$

To prove the well-posedness of this mixed formulation, we again have to check the following two properties. First, the bilinear form a_r is coercive on the kernel $\mathcal{N}_h(b) \coloneqq \{\varphi_h \in \mathbf{\Phi}_h;\ b(\varphi_h,\lambda_h) = 0,\ \forall \lambda_h \in \mathbf{\Lambda}_h\}$. Actually, from the relation

$$a_r(\varphi,\varphi) \geq \min(1, r/\tau)\|\varphi\|^2_{\mathbf{\Phi}}, \quad \forall \varphi \in \mathbf{\Phi},$$

the form a_r is coercive on the full space $\mathbf{\Phi}$, and so a fortiori on $\mathcal{N}_h(b) \subset \mathbf{\Phi}_h \subset \mathbf{\Phi}$. The second property is a discrete inf-sup condition, there exists a constant $\delta_h > 0$ such that

$$\inf_{\lambda_h \in \mathbf{\Lambda}_h} \sup_{\varphi_h \in \mathbf{\Phi}_h} \frac{b(\varphi_h, \lambda_h)}{\|\varphi_h\|_{\mathbf{\Phi}_h} \|\lambda_h\|_{\mathbf{\Lambda}_h}} \geq \delta_h. \tag{21}$$

The spaces $\mathbf{\Phi}_h$ and $\mathbf{\Lambda}_h$ are finite-dimensional, so the infimum and the supremum in (21) are reached. Moreover, from the properties of a_r and with the finite element spaces $\mathbf{\Phi}_h$, $\mathbf{\Lambda}_h$ chosen below, it is standard to prove that δ_h is strictly positive. Consequently, for any $h > 0$, there exists a unique couple $(\varphi_h, \lambda_h) \in \mathbf{\Phi}_h \times \mathbf{\Lambda}_h$ solution of the discrete mixed formulation (21).

On the other hand, if we could show that $\inf_{h>0} \delta_h > 0$, it would ensure the convergence of the solution (φ_h, λ_h) of the discrete formulation (20) towards the solution (φ, λ) of the continuous formulation (18). However, this property is usually difficult to prove and depends strongly on the choice made for the spaces $\mathbf{\Phi}_h$, $\mathbf{\Lambda}_h$. We analyse numerically this property in Section 3.3.

Let us consider a triangulation $\mathcal{T}_h$ of Q_T, i.e. $\cup_{K \in \mathcal{T}_h} K = \overline{Q_T}$. We denote $h \coloneqq \max\{\mathrm{diam}(K);\ K \in \mathcal{T}_h\}$, where $\mathrm{diam}(K)$ is the diameter of the triangle K. In what follows, the space-time mesh $\mathcal{T}_h$ is built from a discretization of the border of Q_T and the curve γ (see Figure 5). Thus, the fineness of $\mathcal{T}_h$ will be given either by h or by the number $N_{\mathcal{T}}$ of vertices per unit of length. This also means that some vertices are supported on γ, making the mesh well-adapted to the control trajectory. The mesh is generated using the software FreeFEM++ (see [17]).

The finite-dimensional space $\mathbf{\Phi}_h$ must be chosen such that $L\varphi_h$ belongs to $L^2(0,T;L^2(\Omega))$, for any $\varphi_h \in \mathbf{\Phi}_h$. Therefore, any space of functions continuously differentiable with respect to both x and t is a conformal approximation of $\mathbf{\Phi}$. We define the space $\mathbf{\Phi}_h$ as follows

$$\mathbf{\Phi}_h \coloneqq \left\{ \varphi_h \in C^1(\overline{Q_T});\quad \varphi_{h|_K} \in \mathbb{P}(K),\ \forall K \in \mathcal{T}_h,\quad \varphi_h = 0 \text{ on } \Sigma_T \right\} \subset \mathbf{\Phi},$$

where $\mathbb{P}(K)$ stands for the complete *Hsieh-Clough-Tocher* finite element (HCT for short) of class C^1. It is a so-called composite finite element. It involves 12 degrees of freedom which are, for each triangle K, the values of φ_h, $\varphi_{h,x}$, $\varphi_{h,t}$ on the three vertices, and the values of the normal derivative of φ in the middle of the three edges. We refer to [12] and [5, 28] for the precise definition and the implementation of such finite element. We also introduce the finite-dimensional space

$$\mathbf{\Lambda}_h \coloneqq \left\{ \lambda_h \in C^0(\overline{Q_T});\quad \lambda_{h|_K} \in \mathbb{Q}(K),\ \forall K \in \mathcal{T}_h,\quad \lambda_h = 0 \text{ on } \Sigma_T \right\} \subset \mathbf{\Lambda},$$

where $\mathbb{Q}(K)$ is the space of affine functions in both x and t on the element K.

Let $n_h = \dim(\mathbf{\Phi}_h)$ and $m_h = \dim(\mathbf{\Lambda}_h)$. We define the matrices $A_{r,h} \in \mathbb{R}^{n_h,n_h}$, $B_h \in \mathbb{R}^{m_h,n_h}$, $M_h \in \mathbb{R}^{m_h,m_h}$ and the vector $L_h \in \mathbb{R}^{n_h}$ by

$$\begin{aligned}
&\langle A_{r,h}\{\varphi_h\}, \{\overline{\varphi}_h\}\rangle = a_r(\varphi_h, \overline{\varphi}_h), && \forall \varphi_h, \overline{\varphi}_h \in \mathbf{\Phi}_h,\\
&\langle B_h\{\varphi_h\}, \{\lambda_h\}\rangle = b(\varphi_h, \lambda_h), && \forall \varphi_h \in \mathbf{\Phi}_h, \forall \lambda_h \in \mathbf{\Lambda}_h,\\
&\langle M_h\{\lambda_h\}, \{\overline{\lambda}_h\}\rangle = \langle \lambda_h, \overline{\lambda}_h\rangle_{\mathbf{\Lambda}}, && \forall \lambda_h, \overline{\lambda}_h \in \mathbf{\Lambda}_h,\\
&\langle L_h, \{\varphi_h\}\rangle = \ell(\varphi_h), && \forall \varphi_h \in \mathbf{\Phi}_h,
\end{aligned}$$

where $\{\varphi_h\} \in \mathbb{R}^{n_h}$ and $\{\lambda_h\} \in \mathbb{R}^{m_h}$ denote the vectors associated with $\varphi_h \in \mathbf{\Phi}_h$ and $\lambda_h \in \mathbf{\Lambda}_h$ respectively. With these notations, the discrete mixed formulation (20) reads as follows: find $\{\varphi_h\} \in \mathbb{R}^{n_h}$ and $\{\lambda_h\} \in \mathbb{R}^{m_h}$ such that

$$\begin{pmatrix} A_{r,h} & -B_h^T \\ -B_h & 0 \end{pmatrix} \begin{pmatrix} \{\varphi_h\} \\ \{\lambda_h\} \end{pmatrix} = \begin{pmatrix} L_h \\ 0 \end{pmatrix}. \tag{22}$$

For any $r > 0$, the matrix $A_{r,h}$ is symmetric and positive definite. However, the matrix in (22) is symmetric but not positive definite. The system (22) is solved by the LU method with FreeFEM++ (see [17]).

3.3 Discrete inf-sup test

Here, we test numerically the discrete inf-sup condition (21), and more precisely the property $\inf_{h>0} \delta_h > 0$. For simplicity, we take $\tau = r > 0$ in (16), so that $a_{r,h}(\varphi, \overline{\varphi}) = \langle \varphi, \overline{\varphi}\rangle_{\mathbf{\Phi}}$ for all $\varphi, \overline{\varphi} \in \mathbf{\Phi}$. It is readily seen (see [10]) that the discrete inf-sup constant satisfies

$$\delta_h = \inf\Big\{\sqrt{\mu};\quad B_h A_{r,h}^{-1} B_h^T\{\lambda_h\} = \mu\, M_h\{\lambda_h\},\ \forall \{\lambda_h\} \in \mathbb{R}^{m_h} \setminus \{0\}\Big\}. \tag{23}$$

For any $h > 0$, the matrix $B_h A_{r,h}^{-1} B_h^T$ is symmetric and positive definite, so the constant δ_h is strictly positive. The generalized eigenvalue problem (23) is solved by the inverse power method (see [11]). Given $\{u_h^0\} \in \mathbb{R}^{m_h}$ such that $\|\{u_h^0\}\|_2 = 1$, for any $n \in \mathbb{N}$, compute iteratively $(\{\varphi_h^n\}, \{\lambda_h^n\}) \in \mathbb{R}^{n_h} \times \mathbb{R}^{m_h}$ and $\{u_h^{n+1}\} \in \mathbb{R}^{m_h}$ as follows

$$\begin{cases} A_{r,h}\{\varphi_h^n\} - B_h^T\{\lambda_h^n\} = 0, \\ B_h\{\varphi_h^n\} = M_h\{u_h^n\}, \end{cases} \qquad \{u_h^{n+1}\} = \frac{\{\lambda_h^n\}}{\|\{\lambda_h^n\}\|_2}.$$

The discrete inf-sup constant δ_h is then given by $\delta_h = \lim_{n\to\infty} \|\{\lambda_h^n\}\|_2^{-\frac{1}{2}}$.

We now compute δ_h for decreasing values of the fineness h, and for different values of the parameter r, namely $r = 10^{-2}$, $r = h$ and $r = h^2$. We use the control

trajectory γ defined in (**Ex1**–γ). The values that we obtain are collected in Table 1. In view of the results for $r = 10^{-2}$, the constant δ_h does not seem to be uniformly bounded by below as $h \to 0$. Thus, we may conclude that the finite elements used here do not "pass" the discrete inf-sup test. As we shall see in the next section, this fact does not prevent the convergence of the sequences $(\varphi_h)_{h>0}$ and $(\lambda_h)_{h>0}$, at least for the cases we have considered. Interestingly, we also observe that δ_h remains bounded by below with respect to h when r depends appropriately on h, as for instance in the case $r = h^2$.

h ($\times 10^{-2}$)	6.46	3.51	2.66	2.17	1.37	1.21
$r = 10^{-2}$	1.8230	1.7947	1.7845	1.6749	1.6060	1.5008
$r = h$	1.4575	1.3806	1.3269	1.2402	1.4188	1.3851
$r = h^2$	1.8873	1.8885	1.8783	1.8697	1.8982	1.8920

Tab. 1: Discrete inf-sup constant δ_h w.r.t. h and r, for γ defined in (**Ex1**–γ).

4 Numerical simulations

In this section, we solve on various examples the discrete mixed formulation (20) to compute the HUM control for (1) and the associated controlled state. First, we determine the rate of convergence of the approximated control/controlled state, as the discretization parameter h goes to zero. Second, for stationary control points $\gamma \equiv x_0$, we illustrate the blow-up of the cost of control at non-strategic points. Finally, we introduce a gradient-type algorithm to solve the problem (12) of optimizing the support of control. The algorithm is then tested on two different initial data. From now on, we set $T = 2$ and $r = 10^{-2}$.

4.1 Convergence of the approximated control

In order to measure the rate of convergence of the approximated control with respect to the mesh fineness h, we use the initial datum

$$y_0(x) = \sin(\pi x), \quad y_1(x) = 0, \quad \forall x \in \Omega, \tag{**Ex1**–$\mathbf{y}_0$}$$

and the control trajectory

$$\gamma(t) = \frac{1}{5} + \frac{3}{5}\frac{t}{T}, \quad \forall t \in [0, T]. \tag{**Ex1**–γ}$$

This curve γ is an admissible trajectory (see [8, Example 3.2]), i.e. the system (1) is controllable. To compare with the approximated solution (φ_h, λ_h) of (20),

using the optimality condition (8), we compute another approximation (φ, λ) by Fourier expansion (see Appendix A), with $N_F = 100$ harmonics. We then evaluate the errors $\|\varphi(\gamma,\cdot) - \varphi_h(\gamma,\cdot)\|_{\mathbf{H}}$ and $\|\lambda - \lambda_h\|_{\mathbf{\Lambda}}$ for the six levels of fineness $N_{\mathcal{T}} = 25, 50, 75, 100, 125, 150$. We gather the results in Table 2 and display them in Figure 1. By linear regression, we find a convergence rate in $h^{0.44}$ for φ_h and in $h^{0.48}$ for λ_h. In Figure 3, we represent the adjoint state φ_h and the controlled state λ_h, for $N_{\mathcal{T}} = 150$. The HUM control v_h computed from φ_h by (9) is shown in Figure 2, together with the "exact" control v obtained by Fourier expansion.

$N_{\mathcal{T}}$	25	50	75	100	125	150
h $(\times 10^{-2})$	6.46	3.51	2.66	1.72	1.40	1.28
$\|\varphi(\gamma,\cdot) - \varphi_h(\gamma,\cdot)\|_{\mathbf{H}}$ $(\times 10^{-1})$	2.15	1.59	1.31	1.20	1.09	1.01
$\|\lambda - \lambda_h\|_{\mathbf{\Lambda}}$ $(\times 10^{-2})$	11.0	8.06	6.69	6.05	5.38	4.81

Tab. 2: (**Ex1**) – Error on the approximated solution (φ_h, λ_h) of (20) w.r.t. h.

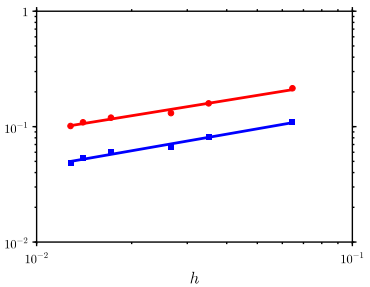

Fig. 1: (**Ex1**) – Error on the approximated solution (φ_h, λ_h) of (20) vs. h – $\|\varphi(\gamma,\cdot) - \varphi_h(\gamma,\cdot)\|_{\mathbf{H}}$ (●), $\|\lambda - \lambda_h\|_{\mathbf{\Lambda}}$ (■).

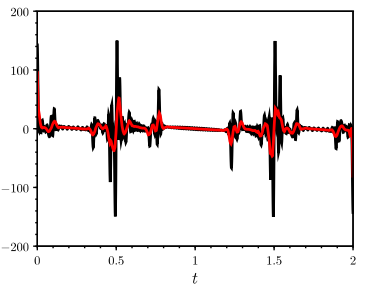

Fig. 2: (**Ex1**) – Controls v_h (–) and v (–), for $N_{\mathcal{T}} = 150$.

4.2 Blow-up at non-strategic points

In the case of a stationary control point $\gamma \equiv x_0 \in \Omega$, it is well-known that one has to choose a so-called strategic point (see [26]) to ensure the controllability of (1). A point x_0 is strategic if and only if $\sin(p\pi x_0) \neq 0$ for every $p \geq 1$. Moreover, a given initial datum $(y_0, y_1) \in \mathbf{V}$ can be controlled if and only if $\sin(p\pi x_0) \neq 0$ for every $p \geq 1$ such that one of the Fourier coefficients $c_p(y_0), c_p(y_1)$ are non-zero.

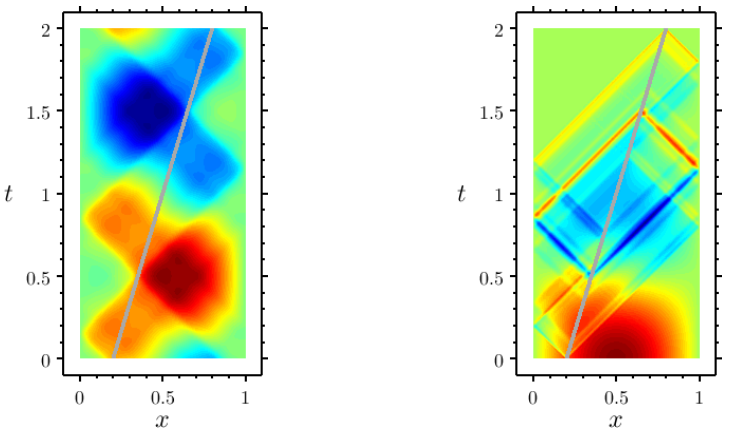

Fig. 3: (Ex1) – Iso-values of the adjoint state φ_h (left) and controlled state λ_h (right), for $N_{\mathcal{T}} = 150$.

Therefore, for $(y_0, y_1) \in \mathbf{V}$ fixed, we expect the cost of control to blow up as x_0 gets closer to a non-strategic location. To illustrate this property, we use the initial datum

$$y_0(x) = \sin(2\pi x), \quad y_1(x) = 0, \quad \forall x \in \Omega, \qquad (\mathbf{Ex2}\text{–}\mathbf{y}_0)$$

and we evaluate the functional $J(x_0)$ (cf. (11)) for several control locations x_0 spread in the interval $(\frac{1}{4}, \frac{1}{2})$. With the initial datum considered, $x^\star = \frac{1}{2}$ is the unique non-strategic point. In Figure 4, we display $J(x_0)$ w.r.t. the distance $|x^\star - x_0|$. As expected, we note that the cost of control blows up when $x_0 \to x^\star$. More precisely, we have $J(x_0) \sim_{x^\star} C_0 |x^\star - x_0|^{-1.97}$.

4.3 Optimization of the support using splines

We now focus on solving numerically the problem (12) with a gradient-type algorithm. To do so, the control trajectories γ considered are degree 5 splines adapted to a fixed subdivision of $[0, T]$. For any integer $N \geq 1$, we denote $S_N = (t_i)_{0 \leq i \leq N}$ the regular subdivision of $[0, T]$ in N intervals. With $\kappa = T/N$, the subdivision points are $t_i = i\,\kappa$. In the simulations below, we use $N = 20$. We then define the set $\mathcal{S}_5$ of degree 5 splines adapted to the subdivision S_N. Such a spline $\gamma \in \mathcal{S}_5$ is of class $C^2([0, T])$ and is uniquely determined by the $3(N + 1)$ conditions

$$\gamma(t_i) = x_i, \quad \gamma'(t_i) = p_i, \quad \gamma''(t_i) = c_i, \quad 0 \leq i \leq N,$$

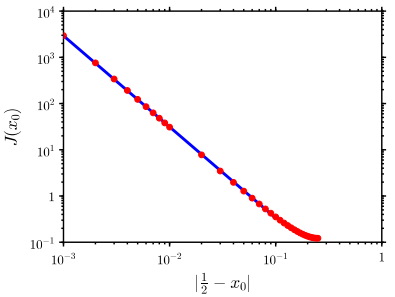

Fig. 4: (Ex2) – $J(x_0)$ vs. $|x^\star - x_0|$, for stationary control points x_0.

where $\mathbf{x} = (x_i)_{0\le i\le N}$, $\mathbf{p} = (p_i)_{0\le i\le N}$ and $\mathbf{c} = (c_i)_{0\le i\le N}$ represent the spline parameters. We also introduce the degree 5 polynomial basis $(P_{k,l})_{\substack{k=0,1,2\\l=0,1}}$ on $[0,1]$ characterized by

$$P_{k,l}^{(k')}(l') = \delta_{k,k'}\,\delta_{l,l'}, \quad \text{for } k,k' \in \{0,1,2\},\ l,l' \in \{0,1\}.$$

Here, $P_{k,l}^{(k')}$ stands for the k'-th derivative of $P_{k,l}$ and $\delta_{k,k'}$ is the Kronecker delta, i.e. $\delta_{k,k'} = 1$ if $k = k'$ and $\delta_{k,k'} = 0$ otherwise. For the sake of presentation, we briefly rename the parameters $(\mathbf{x},\mathbf{p},\mathbf{c}) = (\mathbf{s}^0,\mathbf{s}^1,\mathbf{s}^2)$. It allows to decompose γ into

$$\gamma(t) = \sum_{i=1}^{N}\sum_{k=0}^{2}\left(\mathbf{s}_{i-1}^k P_{k,0}^i(t) + \mathbf{s}_i^k P_{k,1}^i(t)\right)\mathbb{1}_{[t_{i-1},t_i]}(t), \quad \forall t\in[0,T],$$

where we have set $P_{k,l}^i(t) = \kappa^k P_{k,l}\left(\frac{t-t_{i-1}}{\kappa}\right)$. With this decomposition, the optimization problem (12) is reduced to a finite-dimensional problem in the space of parameters, i.e.

$$\min_{\gamma\in\mathcal{S}_5} J_{\varepsilon,\eta}(\gamma) = \min_{\mathbf{s}} \widetilde{J}_{\varepsilon,\eta}(\mathbf{s}), \quad \text{where } \mathbf{s} = (\mathbf{x},\mathbf{p},\mathbf{c}) \in \mathbb{R}^{3(N+1)}.$$

In order to get a descent direction for $J_{\varepsilon,\eta}$ at $\gamma\in\mathcal{S}_5$, we consider the following variational problem: find $j_\gamma \in \mathcal{S}_5$ solution of

$$\begin{aligned}\langle j_\gamma,\overline{\gamma}\rangle_{\mathbf{H}} + \varepsilon\langle j_\gamma'',\overline{\gamma}''\rangle_{L^2(0,T)} = {}& \mathrm{d}J(\gamma;\overline{\gamma}) + \varepsilon\langle\gamma'',\overline{\gamma}''\rangle_{L^2(0,T)}\\ &+ \eta(L(\gamma)-\overline{L})^+\mathrm{d}L(\gamma;\overline{\gamma}), \quad \forall\overline{\gamma}\in\mathcal{S}_5.\end{aligned} \tag{24}$$

Indeed, using Lemma 3, we can see that $\mathrm{d}J_{\varepsilon,\eta}(\gamma;j_\gamma) = \|j_\gamma\|_{\mathbf{H}}^2 + \varepsilon\|j_\gamma''\|_{L^2(0,T)}^2 \ge 0$. The problem (24) is solved by the finite element method using FreeFEM++. We denote by P_Ω the projection in Ω. Then, the gradient algorithm for solving (12) is

given by Algorithm 1. We point out that a re-meshing of Q_T is performed at each iteration, in order to be conform with the current trajectory γ_n. We illustrate the algorithm on two examples.

Algo. 1: Gradient descent

Initialization Choose a trajectory $\gamma_0 \in \mathcal{S}_5$ such that $0 < \gamma_0 < 1$.

For each $n \geq 0$ **do**

- ▷ Compute the solution φ_h of (20) associated with γ_n.
- ▷ Evaluate the costs $J(\gamma_n)$ and $J_{\varepsilon,\eta}(\gamma_n)$.
- ▷ Compute the solution j_{γ_n} of (24).
- ▷ Update the trajectory γ_n by setting

$$\gamma_{n+1} = P_\Omega(\gamma_n - \rho\, j_{\gamma_n}), \quad \text{with } \rho > 0 \text{ fixed.}$$

End

Example 1 – Sine function

To test Algorithm 1, we first use the initial datum

$$y_0(x) = 10\sin(\pi x), \quad y_1(x) = 0, \quad \forall x \in \Omega. \tag{\textbf{Ex3}–$\mathbf{y}_0$}$$

We initialize the algorithm with the trajectory $\gamma_0 \in \mathcal{S}_5$ associated with the parameters

$$x_i = \frac{3}{20} + \frac{1}{5}\frac{t_i}{T}, \quad p_i = \frac{1}{5T}, \quad c_i = 0, \quad 0 \leq i \leq N. \tag{\textbf{Ex3}–γ_0}$$

We set $\varepsilon = 10^{-4}$, $\eta = 10^3$, $\overline{L} = 2.01$ and $\rho = 10^{-2}$. The initial trajectory γ_0, the optimal trajectory $\gamma^\star$ and the optimal controlled state $\lambda^\star$ are displayed in Figure 5. We observe that the optimal trajectory we get is close to a stationary control point located in $x_0 = \frac{1}{2}$, the maximum point of $\sin(\pi x)$. This is coherent with the case of controls distributed over domains $q \subset Q_T$ (see [6, Example **EX1**]).

Example 2 – Travelling wave

To test again the similarities between the pointwise control case and the distributed control case, we now use the initial datum

$$y_0(x) = (10x-3)^2(10x-7)^2\mathbb{1}_{[0.3,0.7]}(x), \quad y_1(x) = y_0'(x), \quad \forall x \in \Omega. \tag{\textbf{Ex4}–$\mathbf{y}_0$}$$

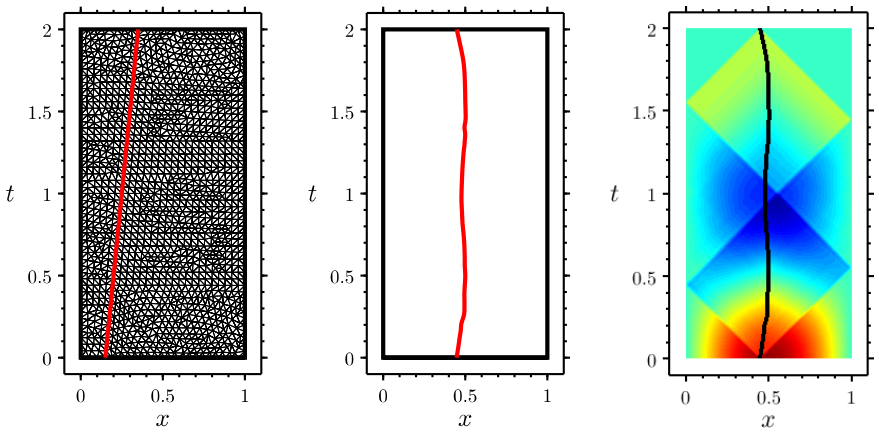

Fig. 5: (Ex3) – Initial trajectory γ_0, optimal trajectory $\gamma^\star$ and optimal controlled state $\lambda^\star$ (from left to right). The left figure also illustrates the type of mesh used to solve (20).

To see whether the control trajectory is likely to "follow" the wave associated with (**Ex4**–$\mathbf{y}_0$) as it is the case in [6, Example **EX2**]), we define the trajectories

$$g_{x_0}(t) = f_{x_0}(t) + 0.15\cos(5\pi(t - x_0)), \quad \text{for any } x_0 \in \Omega.$$

Here, f_{x_0} is the characteristic line "$x+t = x_0$" of the wave equation. The trajectory $g_{\frac{1}{2}}$ is displayed in Figure 8-left. Then, for several values of x_0 in Ω, we evaluate the functional $J(g_{x_0})$ associated with the initial datum (**Ex4**–$\mathbf{y}_0$). The results are displayed in Figure 6, and we can see that J reaches its minimum for $x_0 = \frac{1}{2}$.

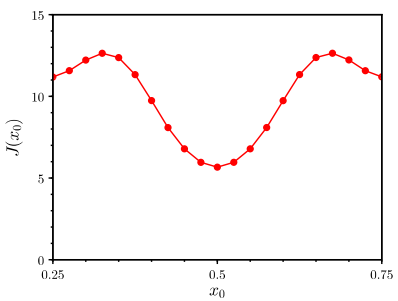

Fig. 6: (Ex4) – $J(g_{x_0})$ vs. x_0.

We then employ Algorithm 1 for two different initial trajectories $\gamma_0 \in \mathcal{S}_5$, respectively defined by

$$x_i = g_{\frac{1}{2}}(t_i), \quad p_i = g'_{\frac{1}{2}}(t_i), \quad c_i = g''_{\frac{1}{2}}(t_i), \quad 0 \le i \le N, \qquad (\textbf{Ex4.1}\text{–}\gamma_0)$$

$$x_i = \frac{1}{4} + \frac{1}{2}\frac{t_i}{T}, \quad p_i = \frac{1}{2T}, \quad c_i = 0, \quad 0 \le i \le N. \qquad (\textbf{Ex4.2}\text{–}\gamma_0)$$

We set $\varepsilon = 10^{-4}$, $\eta = 10^3$, $\overline{L} = 4$ and $\rho = 10^{-2}$. For the two examples (**Ex4.1**) and (**Ex4.2**), we display the initial trajectory γ_0, the optimal trajectory $\gamma^\star$ and the optimal controlled state $\lambda^\star$ in Figures 8-9 respectively. In the first setup, we observe that the optimal trajectory remains close to the wave support, which is coherent with the distributed control case. In the second setup, the optimal trajectory also seems to get closer to the wave support, but the convergence is very slow. This can be seen in Figure 7, where the evolution of the functional $J(\gamma_n)$ and the curve length $L(\gamma_n)$ are shown. The optimal costs are respectively $J(\gamma^\star) = 3.92$ for (**Ex4.1**) and $J(\gamma^\star) = 3.69$ for (**Ex4.2**). The difference is negligible compared to the initial cost $J(\gamma_0) = 37.45$ for the example (**Ex4.2**).

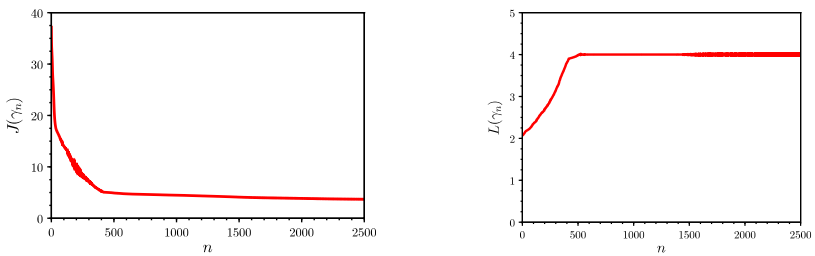

Fig. 7: (**Ex4.2**) – Functional $J(\gamma_n)$ (left) and curve length $L(\gamma_n)$ (right).

5 Conclusion

On the basis of [9] that deals with controls distributed over non-cylindrical domains, we have built a mixed formulation characterizing the HUM control acting on a moving point. The formulation involves the adjoint state and a Lagrange multiplier which turns out to coincide with the controlled state. This approach leads to a variational formulation over a Hilbert space without distinction between the space

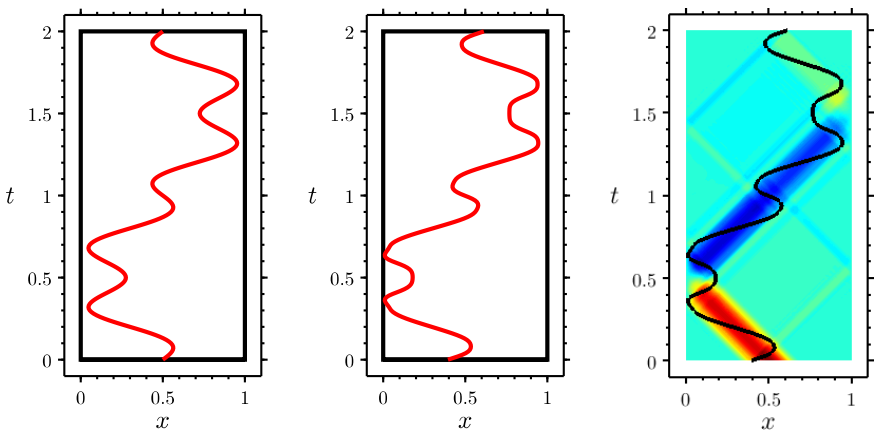

Fig. 8: (**Ex4.1**) – Initial trajectory γ_0, optimal trajectory $\gamma^\star$ and optimal controlled state $\lambda^\star$ (from left to right).

and time variables, making it very appropriate to our moving point situation. We have shown the well-posedness of the formulation using the observability inequality proved in [8]. At a practical level, the mixed formulation is discretized and solved in the finite element framework. The resolution amounts to solve a sparse symmetric system. From a numerical point of view, we have provided evidence of the convergence of the approximated control for regular initial data.

Still from a numerical perspective, for a fixed initial datum, we have considered the natural problem of optimizing the support of control. We have solved this problem with a simple gradient algorithm. For simplicity, the optimization is made over very regular trajectories. The results we get are similar with those obtained in [6], where the same problem is studied for controls distributed over non-cylindrical domains. Although, the convergence towards the optimal trajectory seems to be generally much slower.

This work may be extended to several directions. First, as it is done in [30] for distributed controls, one could try to justify rigorously the well-posedness of the support optimization problem. In that context, it could be interesting to find the minimal regularity necessary for the control trajectories. Besides, one could try to implement other types of algorithm for solving the problem, as for instance an algorithm based on the level-set method. Another challenge is the extension of the observability inequality to the multidimensional case, where we cannot make use of the d'Alembert formula.

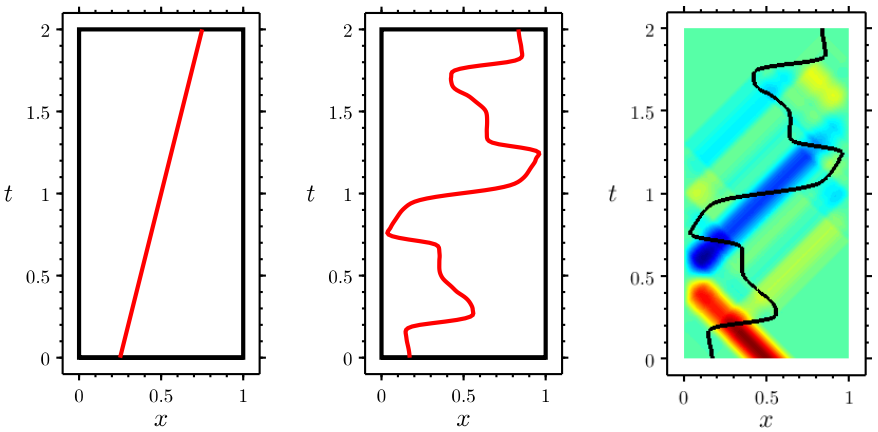

Fig. 9: (**Ex4.2**) – Initial trajectory γ_0, optimal trajectory $\gamma^\star$ and optimal controlled state $\lambda^\star$ (from left to right).

A Fourier expansion of the HUM control

In this appendix, we expand in terms of Fourier series the adjoint state φ linked to the HUM control v by the relation (9), as well as the associated controlled state y. These expansions are used to evaluate the errors $\|v - v_h\|_{\mathbf{H}'}$ and $\|y - y_h\|_{\mathbf{\Lambda}}$ in Section 4. One can show that φ and y take the form

$$\varphi(x,t) = \sum_{p\geq 1} \left(a_p \cos(p\pi t) + \frac{b_p}{p\pi} \sin(p\pi t) \right) \sin(p\pi x), \tag{25}$$

$$y(x,t) = \sum_{p\geq 1} c_p(t) \sin(p\pi x). \tag{26}$$

We set

$$\begin{cases} \xi_p^a(t) = \cos(p\pi t)\sin(p\pi\gamma(t)), \\ \xi_p^b(t) = \dfrac{1}{p\pi}\sin(p\pi t)\sin(p\pi\gamma(t)), \end{cases} \quad \forall p \geq 1.$$

Injecting (25) in the terms appearing in the optimality condition (8), we get

$$\begin{aligned} \int_0^T \varphi(\gamma(t),t)\overline{\varphi}(\gamma(t),t)\,\mathrm{d}t = &\sum_{p,q\geq 1} a_p\overline{a}_q \int_0^T \xi_p^a\xi_q^a + \sum_{p,q\geq 1} b_p\overline{b}_q \int_0^T \xi_p^b\xi_q^b \\ &+ \sum_{p,q\geq 1} a_p\overline{b}_q \int_0^T \xi_p^a\xi_q^b + \sum_{p,q\geq 1} b_p\overline{a}_q \int_0^T \xi_p^b\xi_q^a, \end{aligned} \tag{27}$$

$$\int_0^T \frac{\mathrm{d}}{\mathrm{d}t}\varphi(\gamma(t),t)\frac{\mathrm{d}}{\mathrm{d}t}\overline{\varphi}(\gamma(t),t)\,\mathrm{d}t = \sum_{p,q\geq 1} a_p\overline{a}_q \int_0^T \xi_p^{a\,\prime}\xi_q^{a\,\prime} + \sum_{p,q\geq 1} b_p\overline{b}_q \int_0^T \xi_p^{b\,\prime}\xi_q^{b\,\prime} + \sum_{p,q\geq 1} a_p\overline{b}_q \int_0^T \xi_p^{a\,\prime}\xi_q^{b\,\prime} + \sum_{p,q\geq 1} b_p\overline{a}_q \int_0^T \xi_p^{b\,\prime}\xi_q^{a\,\prime}, \tag{28}$$

$$\int_\Omega y_0\overline{\varphi}_1 = \frac{1}{2}\sum_{p\geq 1} c_p(y_0)\overline{b}_p \quad \text{and} \quad \langle y_1, \overline{\varphi}_0\rangle_{-1,1} = \frac{1}{2}\sum_{p\geq 1} c_p(y_1)\overline{a}_p. \tag{29}$$

Here, $c_p(y_0)$ and $c_p(y_1)$ are the Fourier coefficients of y_0 and y_1. Thus, optimality condition (8) can be rewritten

$$\left\langle \mathcal{M}_\gamma \begin{pmatrix} \{a_p\}_{p\geq 1} \\ \{b_p\}_{p\geq 1} \end{pmatrix}, \begin{pmatrix} \{\overline{a}_q\}_{q\geq 1} \\ \{\overline{b}_q\}_{q\geq 1} \end{pmatrix} \right\rangle = \left\langle \mathcal{F}_{\mathbf{y}_0}, \begin{pmatrix} \{\overline{a}_q\}_{q\geq 1} \\ \{\overline{b}_q\}_{q\geq 1} \end{pmatrix} \right\rangle, \ \forall (\overline{a}_q, \overline{b}_q)_{q\geq 1}, \tag{30}$$

where the positive definite matrix $\mathcal{M}_\gamma$ and the vector $\mathcal{F}_{\mathbf{y}_0}$ are obtained from (27-28) and (29) respectively. The resolution of the infinite-dimensional system (30) (reduced to a finite-dimensional one by truncation) provides an approximation of the adjoint state φ linked to the HUM control v by (9).

Injecting (26) in the wave equation (1), we find that $c_p(t)$ satisfies

$$\begin{cases} c_p''(t) + (p\pi)^2 c_p(t) = 2v(t)\sin(p\pi\gamma(t)), \quad \forall t > 0, \\ c_p(0) = c_p(y_0), \quad c_p'(0) = c_p(y_1). \end{cases}$$

We then have

$$c_p(t) = c_p(y_0)\cos(p\pi t) + \frac{c_p(y_1)}{p\pi}\sin(p\pi t) + \frac{2}{p\pi}\int_0^t v(s)\sin(p\pi\gamma(s))\sin(p\pi(t-s))\,\mathrm{d}s.$$

Finally, by integration by parts, we deduce

$$\begin{aligned} c_p(t) = c_p(y_0)\cos(p\pi t) &+ \frac{c_p(y_1)}{p\pi}\sin(p\pi t) \\ &+ \frac{2}{p\pi}\int_0^t \varphi(\gamma(s),s)\sin(p\pi\gamma(s))\sin(p\pi(t-s))\,\mathrm{d}s \\ &- 2\int_0^t \frac{\mathrm{d}}{\mathrm{d}s}\varphi(\gamma(s),s)\sin(p\pi\gamma(s))\cos(p\pi(t-s))\,\mathrm{d}s \\ &+ 2\int_0^t \frac{\mathrm{d}}{\mathrm{d}s}\varphi(\gamma(s),s)\cos(p\pi\gamma(s))\gamma'(s)\sin(p\pi(t-s))\,\mathrm{d}s. \end{aligned}$$

References

[1] A. Agresti, D. Andreucci, and P. Loreti. Observability for the wave equation with variable support in the Dirichlet and Neumann cases. In *International Conference on Informatics in Control, Automation and Robotics*, pages 51–75. Springer, 2018.

[2] A. Bamberger, J. Jaffre, and J.-P. Yvon. Punctual control of a vibrating string: numerical analysis. *Comput. Math. Appl.*, 4(2):113–138, 1978.

[3] C. Bardos, G. Lebeau, and J. Rauch. Sharp sufficient conditions for the observation, control, and stabilization of waves from the boundary. *SIAM J. Control Optim.*, 30(5):1024–1065, 1992.

[4] M. Berggren and R. Glowinski. Controllability issues for flow-related models: a computational approach. Technical report, 1994.

[5] M. Bernadou and K. Hassan. Basis functions for general Hsieh-Clough-Tocher triangles, complete or reduced. *Internat. J. Numer. Methods Engrg.*, 17(5):784–789, 1981.

[6] A. Bottois, N. Cîndea, and A. Münch. Optimization of non-cylindrical domains for the exact null controllability of the 1D wave equation. *To be published*, 2019.

[7] F. Brezzi and M. Fortin. *Mixed and hybrid finite element methods*, volume 15 of *Springer Series in Computational Mathematics*. Springer-Verlag, New York, 1991.

[8] C. Castro. Exact controllability of the 1-D wave equation from a moving interior point. *ESAIM Control Optim. Calc. Var.*, 19(1):301–316, 2013.

[9] C. Castro, N. Cîndea, and A. Münch. Controllability of the linear one-dimensional wave equation with inner moving forces. *SIAM J. Control Optim.*, 52(6):4027–4056, 2014.

[10] D. Chapelle and K.-J. Bathe. The inf-sup test. *Comput. & Structures*, 47(4-5):537–545, 1993.

[11] F. Chatelin. *Eigenvalues of matrices*, volume 71 of *Classics in Applied Mathematics*. Society for Industrial and Applied Mathematics (SIAM), Philadelphia, PA, 2012. With exercises by Mario Ahués and the author, Translated with additional material by Walter Ledermann, Revised reprint of the 1993 edition [MR1232655].

[12] P. Ciarlet. *The finite element method for elliptic problems*, volume 40 of *Classics in Applied Mathematics*. Society for Industrial and Applied Mathematics (SIAM), Philadelphia, PA, 2002. Reprint of the 1978 original [North-Holland, Amsterdam; MR0520174 (58 #25001)].

[13] N. Cîndea and A. Münch. A mixed formulation for the direct approximation of the control of minimal L^2-norm for linear type wave equations. *Calcolo*, 52(3):245–288, 2015.

[14] R. Dáger and E. Zuazua. *Wave propagation, observation and control in* 1*-d flexible multi-structures*, volume 50 of *Mathématiques & Applications (Berlin) [Mathematics & Applications]*. Springer-Verlag, Berlin, 2006.

[15] S. Ervedoza and E. Zuazua. A systematic method for building smooth controls for smooth data. *Discrete Contin. Dyn. Syst. Ser. B*, 14(4):1375–1401, 2010.

[16] R. Glowinski, J.-L. Lions, and J. He. *Exact and approximate controllability for distributed parameter systems*, volume 117 of *Encyclopedia of Mathematics and its Applications*. Cambridge University Press, Cambridge, 2008. A numerical approach.

[17] F. Hecht. New development in freefem++. *J. Numer. Math.*, 20(3-4):251–265, 2012.

[18] A. Henrot, W. Horn, and J. Sokołowski. Domain optimization problem for stationary heat equation. *Appl. Math. Comput. Sci.*, 6(2):353–374, 1996. Shape optimization and scientific computations (Warsaw, 1994).

[19] A. Henrot and J. Sokołowski. A shape optimization problem for the heat equation. In *Optimal control (Gainesville, FL, 1997)*, volume 15 of *Appl. Optim.*, pages 204–223. Kluwer Acad. Publ., Dordrecht, 1998.

[20] A. Khapalov. Controllability of the wave equation with moving point control. *Appl. Math. Optim.*, 31(2):155–175, 1995.

[21] A. Khapalov. Mobile point controls versus locally distributed ones for the controllability of the semilinear parabolic equation. *SIAM J. Control Optim.*, 40(1):231–252, 2001.

[22] A. Khapalov. Observability and stabilization of the vibrating string equipped with bouncing point sensors and actuators. *Math. Methods Appl. Sci.*, 24(14):1055–1072, 2001.

[23] J. Le Rousseau, G. Lebeau, P. Terpolilli, and E. Trélat. Geometric control condition for the wave equation with a time-dependent observation domain. *Anal. PDE*, 10(4):983–1015, 2017.

[24] J.-L. Lions. *Some methods in the mathematical analysis of systems and their control*. Kexue Chubanshe (Science Press), Beijing; Gordon & Breach Science Publishers, New York, 1981.

[25] J.-L. Lions. *Contrôlabilité exacte, perturbations et stabilisation de systèmes distribués. Tome 1*, volume 8 of *Recherches en Mathématiques Appliquées [Research in Applied Mathematics]*. Masson, Paris, 1988. Contrôlabilité exacte. [Exact controllability], With appendices by E. Zuazua, C. Bardos, G. Lebeau and J. Rauch.

[26] J.-L. Lions. Pointwise control for distributed systems. In *Control and estimation in distributed parameter systems*, pages 1–39. SIAM, 1992.

[27] J.-L. Lions and E. Magenes. *Non-homogeneous boundary value problems and applications. Vol. I.* Springer-Verlag, New York-Heidelberg, 1972. Translated from the French by P. Kenneth, Die Grundlehren der mathematischen Wissenschaften, Band 181.

[28] A. Meyer. A simplified calculation of reduced HCT-basis functions in a finite element context. *Comput. Methods Appl. Math.*, 12(4):486–499, 2012.

[29] A. Münch. A uniformly controllable and implicit scheme for the 1-D wave equation. *M2AN Math. Model. Numer. Anal.*, 39(2):377–418, 2005.

[30] F. Periago. Optimal shape and position of the support for the internal exact control of a string. *Systems Control Lett.*, 58(2):136–140, 2009.

[31] Á. M. Ramos, R. Glowinski, and J. Périaux. Pointwise control of the Burgers equation and related Nash equilibrium problems: computational approach. *J. Optim. Theory Appl.*, 112(3):499–516, 2002.